International Journal of Safety and Security Engineering
Vol. 15, No. 10, October, 2025, pp. 2055-2060
Journal homepage: http://iieta.org/journals/ijsse

Pulsed Nd:YAG Laser Ablation: Environmentally Friendly Synthesis of ZnO/TiO_2 Nanocomposites for Wastewater Treatment Applications

Mohammed J. Jader*, Mohammed H.K. Al-Mamoori, Saif M. Alshrefi, Zahraa F. Abd Al-Sada, Zainab F. Abd Al-Sada, Sajjad Abbas Hadi Nukhailawi

Department of Laser Physics, College of Science for Women, University of Babylon, Hilla 51001, Iraq

Corresponding Author Email: Wsci.mohammed.jawad@uobabylon.edu.iq

https://doi.org/10.18280/ijsse.151008

Received: 11 September 2025
Revised: 12 October 2025
Accepted: 23 October 2025
Available online: 31 October 2025

Keywords:
ZnO-TiO_2 nanocomposites, laser ablation, remove pollutants

ABSTRACT

ZnO/TiO_2 nanocomposites were successfully created by ablation with a Q-switched Nd:YAG pulsed laser. To create the nanocomposite, Zn and TiO_2 powders were first compacted into pellets, then ablated in distilled water to create colloidal nanoparticles. These were then combined in a 1:1 volume ratio. X-ray diffraction (XRD) structural investigation verified the production of highly crystalline titanium dioxide (TiO_2) and crystalline zinc oxide (ZnO) in the wurtzite hexagonal phase, with ZnO nanoparticles dominating in the composite. It was found that ZnO and TiO_2 nanoparticles had typical crystallite diameters of 26.9 nm and 19.8 nm, respectively. An average particle size of 63 nm and a polydisperse distribution of nanoparticles with noticeable agglomeration were observed using scanning electron microscopy (SEM). When compared to pure nanoparticles, optical analysis employing UV-visible absorption spectroscopy revealed notable modifications in the nanocomposites' absorption characteristics. Within the nanocomposite, the ZnO nanoparticles showed a redshift in the absorption edge from 395 nm to 627.6 nm, whereas the TiO_2 nanoparticles showed a blueshift in relation to bulk TiO_2. Quantum confinement effects, interfacial charge transfer interactions, and the generation of surface states were indicated by the optical band gaps, which were determined using Tuac plot method to be 2.9 eV for ZnO nanoparticles and 3.18 eV for the ZnO/TiO_2 nanocomposite. Under light irradiation, the degradation of methylene blue (MB) dye was used to assess the ZnO/TiO_2 nanocomposite's photocatalytic potential. The nanocomposite achieved a degrading efficiency of 33.8% and successfully decreased the MB concentration over a 25-second period. Because of the synergistic effects of ZnO and TiO_2 nanoparticles, electron-hole recombination is suppressed, leading to increased photocatalytic activity. Pulsed laser ablation is a successful technique for creating ZnO/TiO_2 nanocomposites with certain structural and optical characteristics, as this study shows overall. The produced nanocomposites show promise for wider use in energy and water treatment technologies through their use in environmental remediation and photocatalysis.

1. INTRODUCTION

Nanocomposites have attracted much attention because of their unique and enhanced properties in relation to their single constituents. Regarding photocatalysts and energy storage materials, also in sensors and optoelectronic devices, two of the most interesting metal oxide nanocomposites are zinc oxide (ZnO) and titanium dioxide (TiO_2). ZnO is a semiconductor with a band gap of 3.37 eV and great photocatalytic activity, which is therefore advantageous for many energy and environmental demanding problems [1, 2]. Another widely-used semiconductor with great chemical stability, photocatalytic activity, and relatively non-toxic character is TiO_2 [3, 4]. The combined ZnO and TiO_2 in a nanocomposite form could provide improved mechanical, optical, and electrical properties as well as more photocatalytic effectiveness due to their synergistic effects [5, 6].

Controlling the shape, crystallinity, and surface properties of a range of ZnO/TiO_2 nanocomposites remains a difficulty in synthesis. Sol-gel, hydrothermal, CVD, and laser-assisted techniques [7, 8] are among the several ways one might prepare the nanocomposites. Of them, laser-based solutions—mostly Q-switched Nd:YAG pulsed lasers—are drawing great interest because of their capabilities. to precisely regulate the nanoparticle size, form, and crystalline composition. One of these methods is pulsed laser ablation in liquids (PLAL), which uses high-energy laser pulses to produce fast heating and nucleation of nanoparticles, therefore boosting the production of ZnO/TiO_2 nanocomposites with tailored properties [9, 10].

Q-switched Nd:YAG pulsed laser is very appealing for this reason: its high pulse energy, short pulse duration, and capacity to produce significant local heating will help to improve nucleation of the particles and their high crystallinity.

With the guiding parameters comprising the laser fluence, pulse duration, and ablation time, which control the final properties of the produced nanocomposite [11, 12], this has allowed the preparation of several metal oxide nanocomposites.

ZnO and TiO_2 in their nanocomposite form have been synthesized using pulsed laser ablation with enhanced photocatalytic activity for various uses, including hydrogen generation and organic pollution degradation [13, 14]. Here, we synthesize ZnO/TiO_2 nanocomposites by means of Q-switched Nd:YAG pulsed ablation of lasers.

The structural, morphological, and optical characteristics of the nanocomposites are the main emphasis of this work. The findings of this research will help to fill some of the knowledge voids around laser-assisted.

2. MATERIALS AND METHODS

2.1 Materials

To prepare the Zn and TiO_2 disc for pulsed laser ablation, Zn and TiO_2 powder are compressed using a hydraulic press.

2.2 Characterization techniques

The morphology of the samples was measured using a JSM-6510LV field emission scanning electron microscope (FE-SEM) (Model S-1640, Hitachi, Japan). The sample structures were analyzed using a Shimadzu 6000 X-ray diffractometer (made in Japan) in reflection geometry using $\lambda = 1.5406$ Å of Cu-Kα radiation. The optical properties of all the prepared materials were determined using a UV-visible absorption spectroscopy (CECIL CE 7200, England).

2.3 Preparation of ZnO/TiO_2 nanocomposites

Pure Zn and TiO_2 pellets were immersed in 10 mL of distilled water in tow separated beakers and ablated using Nd:YAG pulsed laser (wavelength 1064 nm, 4 Hz, 100 mJ, 300 pulses), as shown in the flowchart in Figure 1. The laser beam was focused on the Zn and TiO_2 targets to form ZnO and TiO_2 colloidal nanoparticles, respectively, and their structures and optical properties were subsequently studied. The colloidal solutions of ZnONPs and TiO_2NPs were mixed in a volume ratio of 1:1 to synthesize ZnO/TiO_2 nanocomposites, as shown in the flowchart in Figure 1.

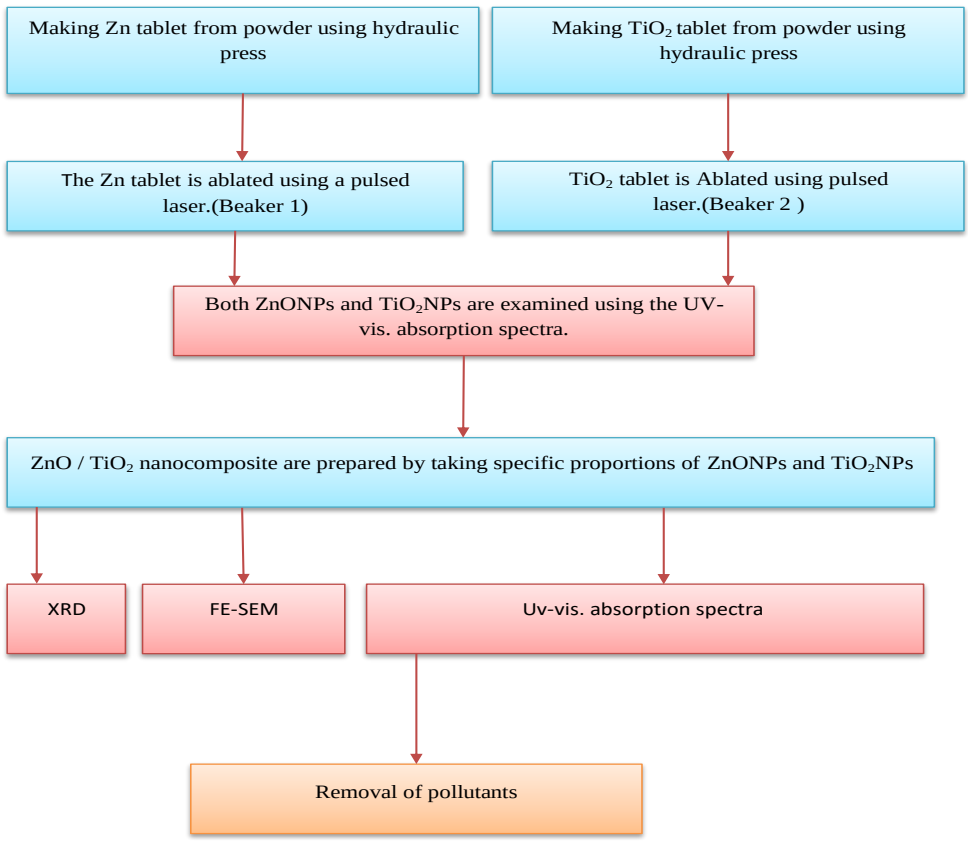

Figure 1. The practical scheme for the preparation of ZnO/TiO_2 nanocomposites using Q-switched Nd:YAG pulsed laser ablation

3. RESULTS AND DISCUSSION

3.1 X-ray reflection results

The X-ray diffraction (XRD) pattern of ZnO/TiO_2 nanocomposites is displayed in Figure 2. Miller indices (100), (002), (101), (110) and (103) corresponding to the diffraction peaks at $2\theta = 33°$, 36.5°, 43.8°, 58.4° and 61.6° respectively as shown in Figure 2 and thereby matching the data of researchers in reference and standard card JCPDS-36-1451 and it's indicated to form Wurtzite hexagonal phase of ZnO [15]. The diffraction peaks at 23.5°, 30.5°, 48.2°, and 50° correspond to Bragg reflection planes (101), (004), (200), and (105) representing the highly crystalline nature of TiO_2 NPs, similar to the information of researchers in reference and standard card JCPDS21-1272 [16]. It is noted that the ZnONPs dominate over TiO_2 NPs in the ZnO/TiO_2 nanocomposites.

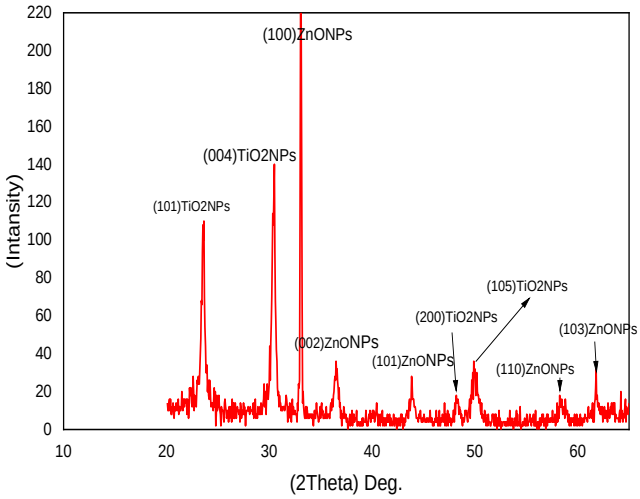

Figure 2. XRD pattern of ZnO/TiO_2 nanocomposite

To calculate the highest peak crystal size of ZnONPs and TiO_2NPs in ZnO/TiO_2 nanocomposites, we applied the Scherrer equation $D = \frac{K\lambda}{\beta \cos\theta}$, where D is the average crystal size, K is a dimensionless shape factor with a value close to 1, λ is the wavelength of X-rays, β is the full width at half maximum (FWHM), and θ is the Bragg angle. The crystal sizes are 26.9 nm and 19.8 nm for ZnONPs and TiO_2NPs, respectively.

The XRD peaks of ZnONPs and TiO_2NPs in a ZnO/TiO_2 nanocomposite do not shift, which usually indicates that the XRD peaks corresponding to the individual ZnO and TiO_2 phases do not change or shift considerably in the composite material when compared to the pure nanoparticles. Particle size effects, physical mixture instead of chemical bonding, and the absence of new phase development are among possible interpretations of this [17]. In the ZnO/TiO_2 nanocomposite, ZnONPs are similarly observed to predominate over TiO_2NPs.

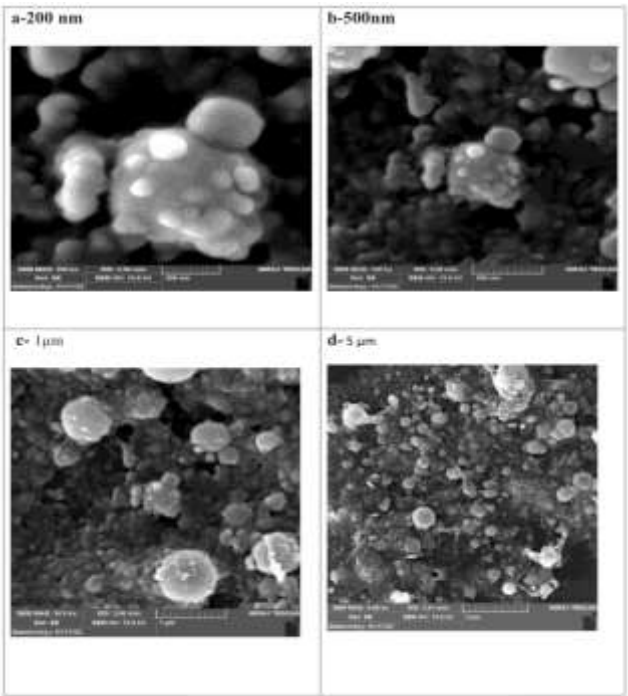

Figure 3. FE-SEM of ZnO/TiO_2 nanocomposite: (a) 200 nm, (b) 500 nm, (c) 1 µm, and (d) 5 µm

3.2 Scanning electron microscopy

Clearly exhibits a collection of nanoparticles of varying sizes and rough shapes. Figure 3 illustrates the obvious agglomeration that exists here. Instead of being uniformly dispersed, the nanoparticles cluster [18, 19]. The polydisperse sample is shown by the range of sizes the particles show. The agglomerate surfaces seem to be somewhat uneven and harsh. Either the agglomeration process itself or the intrinsic shape of the nanoparticles could be to blame. Nanoparticles are clearly visible in the photograph, confirming that a nanocomposite was successfully formed. It is difficult to differentiate ZnONPs from TiO_2NPs only by shape, though.

The average particle size of the ZnO/TiO_2 nanocomposite was calculated using the Image J program and was equal to 63 nm, as shown in Figure 4.

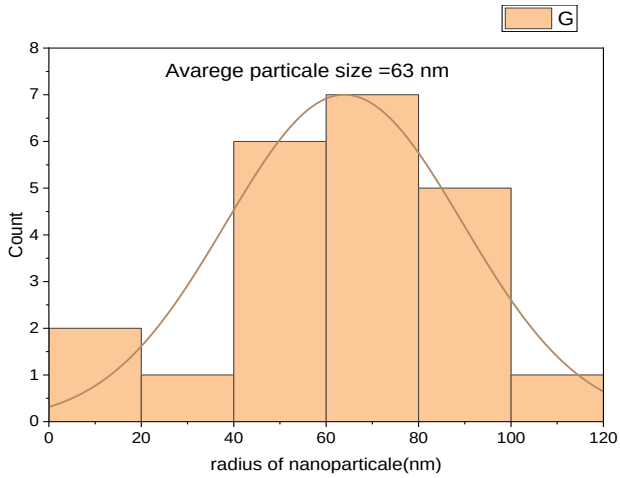

Figure 4. The histogram of ZnO/TiO_2 nanocomposite

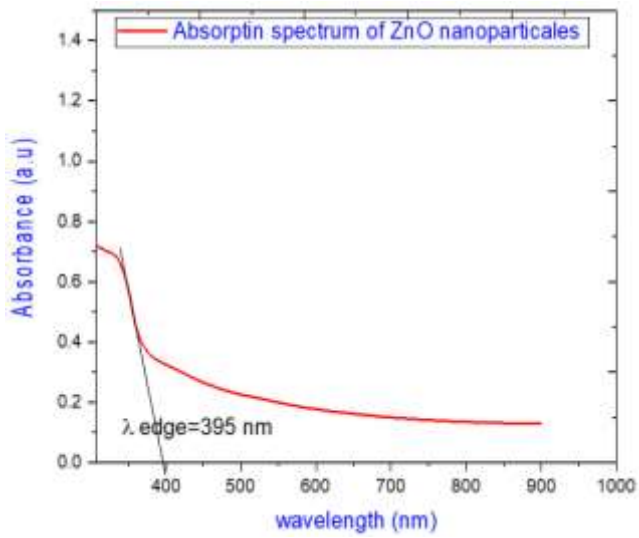

Figure 5. The absorption spectra of ZnONPs

3.3 UV-visible absorbance spectroscopy

The quantum confinement effect of pulsed laser producing a lower band gap relative to bulk ZnO, whose absorption edge is usually closer to 368 nm, causes a shift in ZnONPs absorption edge at 395 nm as shown in Figure 5. Their improved photonic, electrical, and catalytic behaviours depend critically on the change in optical characteristics from bulk to

nanoparticle form. It is consistent with what is mentioned in previous studies [20, 21]. The absorption edge of the ZnONPs undergoes a red shift from 395 nm to 627.6 nm within the nanocomposite, while the absorption peak of the TiO_2NPs undergoes a blue shift in comparison to bulk TiO_2 in the nanocomposite, as shown in Figure 6, and this result is close to what was stated in a previous study [22].

Figure 6 shows the absorption spectrum of the ZnO/TiO_2 nanocomposite. The interactions between nanoparticles, surface states, quantum confinement effects, and matrix material effects mostly determine the red shift in ZnO and the blue shift in TiO_2 employed in nanocomposites. Depending on their inherent electronic characteristics and how these characteristics are changed in the nanocomposite environment, every material reacts differently [23, 24].

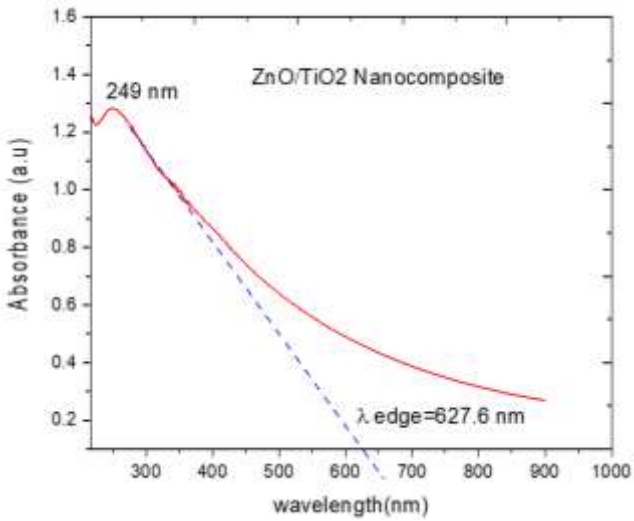

Figure 6. The absorption spectra of ZnO/TiO_2 nanocomposite

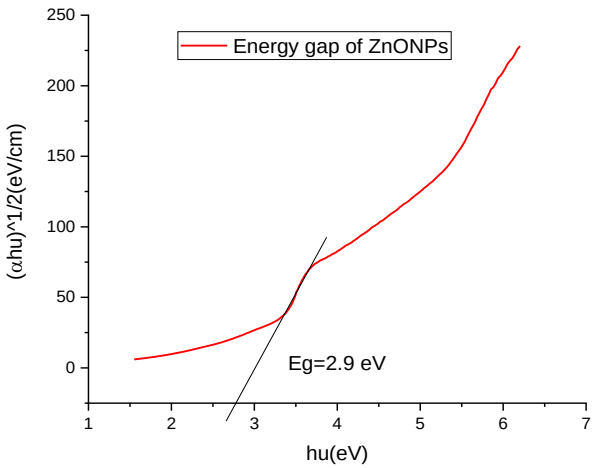

Figure 7. The direct energy gap calculated by Tuac Plot equation of ZnO NPs

The energy gap for both ZnO NPs and ZnO/TiO_2 Nanocomposite was calculated using the Tuac relationship between the absorption coefficient α and the photon energy hυ as written in the following equation:

$$\alpha h\upsilon = A(h\upsilon - E_g)^n$$

where, h is the plank's constant, υ is frequency of the photon, hυ is photon energy in eV, E_g is optical band gap in eV, B is a constant, n is an exponent which is 2 for indirect band transitions and 1/2 for direct band transition and α is the absorption coefficient. When the straight portion of the graph of $\alpha h\nu^2$ against hυ is extrapolated to α = 0, the intercept gives the transition band gap. The photon can interact with a valence electron, elevates the electron into the C.B, and creates an electron–hole pair. The direct energy gap are 2.9 eV and 3.18 eV for ZnONPs and ZnO/TiO_2 nanocomposite, as shown in Figure 7 and Figure 8, respectively.

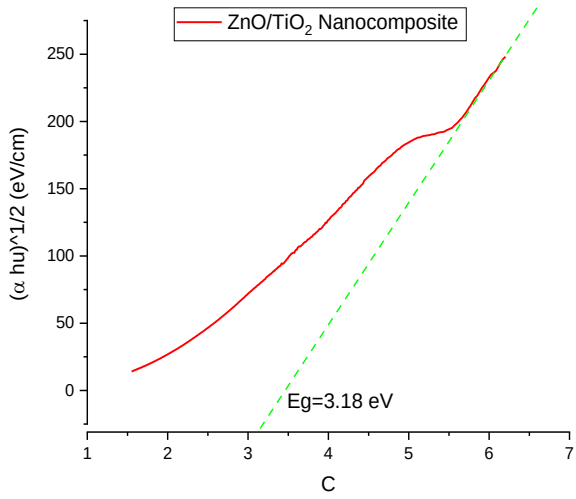

Figure 8. The direct energy gap calculated by Tuac plot equation of ZnO/TiO_2 nanocomposite

Quantum size effects, band alignment at the interface, Charge transfer interactions, the development of surface states and defects at the interface, which influence the electronic properties, the hybridization of electronic states at the interface, and oxygen deficiency (oxygen vacancies) can lead to an increase in the apparent band gap in a nanocomposite compared to the individual materials. These effects together produce a bigger band gap than for single ZnO nanoparticles and this is supported by what the previous studies stated. The size-induced property change of nanostructures has inspired numerous theoretical models [25, 26].

3.4 Removing the methylene blue dye from the water by using the prepared ZnO/TiO_2 nanocomposite

The ZnO/TiO_2 nanocomposite was employed to eliminate methylene blue (MB) pigment, which is employed in the coloring of leather and textiles. The ZnO/TiO_2+MB mixture was manufactured in the following manner: 2.0 ml of the ZnO/TiO_2 nanocomposite was added to 0.1 ml of MB dye with a concentration of (10^{-6} M) in 7.9 ml of distilled water. The absorbance of each ZnO/TiO_2 nanocomposite was determined at t = 0, 5, 10, 15, 20, and 25 seconds, as illustrated in Figure 9. The electronic transitions within the MB molecule are responsible for the prominent peak at approximately 660 nm. The absorbance peak at 660 nm decreases as the irradiation time increases (from 0 s to 25 s). This suggests a decrease in the concentration of MB in the solution. The ZnO/TiO_2 nanocomposite is effectively degrading the MB under light irradiation, as indicated by the decrease in MB concentration. Electrons in the valence band get excited and leap to the conduction band when the ZnO/TiO_2 nanocomposite is subjected to light with energy equivalent to or larger than its

energy gap (UV or visible light), hence creating electron and hole couples. Reaching the MB molecules, the hydroxyl radicals (•OH) and superoxide radicals (O_2^-) break them down into simpler, less toxic compounds (mineralization). Combining ZnO and TiO_2 can lower the recombination rate of photogenerated electron-hole pairs [27-29], thereby enhancing the photocatalytic process's efficiency, and equal to 33.8% as computed from Eq. (1):

$$D.E(\%) = \left(\frac{A_0 - A_t}{A_0}\right) * 100\% \quad (1)$$

Before irradiation, the absorbance of MB is denoted by A_0, while after irradiation for a specific duration, it is denoted by A_t. The behavior of these synthetic nanomaterials in dye adsorption is similar to what researchers reported in the previous studies [30-34].

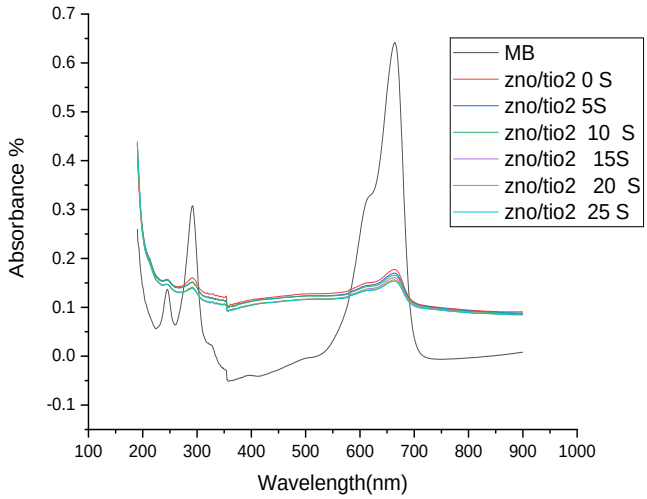

Figure 9. The photodegradation of MB by ZnO/TiO_2 nanocomposite at different times

4. CONCLUSIONS

This study showed that ZnO/TiO_2 nanocomposites could be successfully synthesized using pulsed laser ablation. The XRD study revealed clear peaks that corresponded to the ZnO and TiO_2 phases, confirming the nanocomposites' crystalline structure. With an average particle size of 63 nm, the agglomeration of nanoparticles was seen using scanning electron microscopy (SEM). UV-visible absorbance spectroscopy revealed important optical changes in the nanocomposites: a redshift in the absorption edge of ZnO and a blueshift for TiO_2, attributable to the quantum confinement effect and nanoparticle interactions. The increasing energy gap of the ZnO/TiO_2 nanocomposites (3.18 eV) above pure ZnO (2.9 eV) indicates enhanced photocatalytic performance. This work underlines its fascinating applications in photocatalysis and other fields, in addition to demonstrating that laser ablation is viable for the production of ZnO/TiO_2 nanocomposites. Still under development, is investigating the practical application of these nanocomposites in environmental and energy-related technologies. In this work, the ZnO/TiO_2 nanocomposites were applied in the process of effectively eliminating contaminants like MB dye from water with 33.8% efficiency.

REFERENCES

[1] Manjunatha, C., Rastogi, C.K., Rao, B.M., Kumar, S.G., et al. (2024). Advances in hierarchical inorganic nanostructures for efficient solar energy harvesting systems. ChemSusChem, 17(11): e202301755. https://doi.org/10.1002/cssc.202301755

[2] Tamanna, N.J., Hossain, M.S., Tabassum, S., Bahadur, N.M., Ahmed, S. (2024). Easy and green synthesis of nano-ZnO and nano-TiO_2 for efficient photocatalytic degradation of organic pollutants. Heliyon, 10(17): e37469. https://doi.org/10.1016/j.heliyon.2024.e37469

[3] Nagaraj, K., Radha, S., Deepa, C.G., Raja, K., et al. (2025). Photocatalytic advancements and applications of titanium dioxide (TiO_2): Progress in biomedical, environmental, and energy sustainability. Next Research, 2(1): 100180. https://doi.org/10.1016/j.nexres.2025.100180

[4] Mousa, H.M., Alenezi, J.F., Mohamed, I.M., Yasin, A.S., Hashem, A.F.M., Abdal-Hay, A. (2021). Synthesis of TiO_2@ ZnO heterojunction for dye photodegradation and wastewater treatment. Journal of Alloys and Compounds, 886: 161169. https://doi.org/10.1016/j.jallcom.2021.161169

[5] Ren, X.Q., Niu, J.H., Li, Y., Li, L., Zhang, C., Guo, Q., Zhang, Q.L., Jiao, W.Z. (2024). Photocatalytic ozonation-based degradation of phenol by ZnO-TiO_2 nanocomposites in spinning disk reactor. Chinese Journal of Chemical Engineering, 72: 74-84. https://doi.org/10.1016/j.cjche.2024.03.028

[6] Pinzari, F. (2024). Synthesis, photocatalytic and bio activity of ZnO-TiO_2 nanocomposites: A review study. Reactions, 5(4): 680-739. https://doi.org/10.3390/reactions5040035

[7] Das, S., Dhara, S. (2021). Chemical Solution Synthesis for Materials Design and Thin Film Device Applications. Elsevier.

[8] Jun, W.J.W., Aiman, D.A.A.O.D., Mohammed, D.M.S.N.D., Nusari, S. (2024). Synthesis and characterization of nanoscale iron oxide for environmental uses. Journal of Management and Architecture Research, 6(1): 46-57. https://jomaar.com/index.php/jomaar/article/download/8/8/30.

[9] Eason, R. (2006). Pulsed Laser Deposition of Thin Films: Applications-Led Growth of Functional Materials. John Wiley & Sons. https://doi.org/10.1002/0470052120

[10] Yogesh, G.K., Shukla, S., Sastikumar, D., Koinkar, P. (2021). Progress in pulsed laser ablation in liquid (PLAL) technique for the synthesis of carbon nanomaterials: A review. Applied Physics A, 127(11): 810. https://doi.org/10.1007/s00339-021-04951-6

[11] Ortaç, B., Mutlu, S., Yilmaz, A.H., Arsu, N., Yilmaz, S.S. (2025). Laser-assisted synthesis of metals, metal oxide nanoparticles, and metal-organic frameworks (MOFs): Applications in photocatalysis, batteries, and beyond. IntechOpen. https://doi.org/10.5772/intechopen.1010923

[12] Lan, R., Wang, Z., Liu, H., Yu, H., et al. (2010). Passively Q-switched Nd: YAG ceramic laser towards large pulse energy and short pulse width. Laser Physics, 20(1): 187-191. https://doi.org/10.1134/S1054660X10010093

[13] Iasya, Y.K.A.A., Khoerunnisa, F., Dwi, S.S., Putri, R.A.,

et al. (2025). Synergetic effect of ZnO/NiO nanocomposite on the enhancement of photocatalytic degradation efficiency of dyes molecules. Communications in Science and Technology, 10(1): 1-9. https://doi.org/10.21924/cst.10.1.2025.1583

[14] Al-Janabi, N. (2025). Pulse laser ablation synthesis of Chitosan-ZnO-TiO_2 nanocomposites for bacterial inhibition. Journal of Nanostructures, 15(2): 534-542. https://doi.org/10.22052/JNS.2025.02.014

[15] Habib, M.A., Shahadat, M.T., Bahadur, N.M., Ismail, I.M.I., Mahmood, A.J. (2013). Synthesis and characterization of ZnO-TiO_2 nanocomposites and their application as photocatalysts. International Nano Letters, 3(1): 1-8. https://doi.org/10.1186/2228-5326-3-5

[16] Aravind, M., Amalanathan, M., Michael Mary, M.S. (2021). Synthesis of TiO_2 nanoparticles by chemical and green synthesis methods and their multifaceted properties. SN Applied Sciences, 3: 409. https://doi.org/10.1007/s42452-021-04281-5

[17] Mintcheva, N., Yamaguchi, S., Kulinich, S.A. (2020). Hybrid TiO_2-ZnO nanomaterials prepared using laser ablation in liquid. Materials, 13(3): 719. https://doi.org/10.3390/ma13030719

[18] Rahal, A., Bouchama, I., Ghebouli, M.A., Alanazi, F.K., Ghebouli, B., Fatmi, M., Chihi, T., Althagafi, T.M., Khettab, K. (2025). Experimental investigation of structural and optical properties of Mn-doped ZnO thin films deposited by pneumatic spray technique. Scientific Reports, 15: 7086. https://doi.org/10.1038/s41598-025-90425-1

[19] Waychunas, G.A. (2001). Structure, aggregation and characterization of nanoparticles. Reviews in Mineralogy and Geochemistry, 44(1): 105-166. https://doi.org/10.2138/rmg.2001.44.04

[20] Elsisi, M.E., Mostafa, M.M., Abdella, H., Khalil, A.E., Soror, A.S. (2025). In-depth investigation the size effect of zinc oxide nanostructures on the photodegradation of different dyes under UV-irradiation: Anticancer application. Scientific Reports, 15: 31669. https://doi.org/10.1038/s41598-025-16270-4

[21] Cortie, M.B., McDonagh, A.M. (2011). Synthesis and optical properties of hybrid and alloy plasmonic nanoparticles. Chemical Reviews, 111(6): 3713-3735. https://doi.org/10.1021/cr1002529

[22] Ali, M., Tan, Y., Kadir, S., Lin, F., Su, Z., Liao, W.H., Wong, H. (2025). Generation of titanium dioxide nanoparticles in liquids using laser ablation: Analysing the roles of temperature and viscosity. Materials Science and Engineering: B, 319: 118383. https://doi.org/10.1016/j.mseb.2025.118383

[23] Mofokeng, S.J., Kumar, V., Kroon, R.E., Ntwaeaborwa, O.M. (2017). Structure and optical properties of Dy3+ activated sol-gel ZnO-TiO_2 nanocomposites. Journal of Alloys and Compounds, 711: 121-131. https://doi.org/10.1016/j.jallcom.2017.03.345

[24] Khan, R., Rahman, N., Prasannan, A., Ganiyeva, K., Chakrabortty, S., Sangaraju, S. (2025). Phase transition and bandgap modulation in TiO_2 nanostructures for enhanced visible-light activity and environmental applications. Scientific Reports, 15: 20309. https://doi.org/10.1038/s41598-025-07000-x

[25] Sun, C.Q. (2007). Size dependence of nanostructures: Impact of bond order deficiency. Progress in Solid State Chemistry, 35(1): 1-159. https://doi.org/10.1016/j.progsolidstchem.2006.03.001

[26] Zhong, Z., Hansmann, P. (2017). Band alignment and charge transfer in complex oxide interfaces. Physical Review X, 7(1): 011023. https://doi.org/10.1103/PhysRevX.7.011023

[27] Tuama, A.N., Alzubaidi, L.H., Jameel, M.H., Abass, K.H., bin Mayzan, M.Z.H., Salman, Z.N. (2024). Impact of electron–hole recombination mechanism on the photocatalytic performance of ZnO in water treatment: A review. Journal of Sol-Gel Science and Technology, 110(3): 792-806. https://doi.org/10.1007/s10971-024-06385-x

[28] Giram, D., Das, A., Bhanvase, B. (2023). Comparative study of ZnO-TiO_2 nanocomposites synthesized by ultrasound and conventional methods for the degradation of methylene blue dye. Indian Journal of Chemical Technology (IJCT), 30(5): 693-704. https://doi.org/10.56042/ijct.v30i5.5200

[29] Akhter, P., Nawaz, S., Shafiq, I., Nazir, A., et al. (2023). Efficient visible light assisted photocatalysis using ZnO/TiO_2 nanocomposites. Molecular Catalysis, 535: 112896. https://doi.org/10.1016/j.mcat.2022.112896

[30] Saeed, G., Al-Mamoori, M.H.K., Madluim, K.N. (2023). Study of the optical, structural and adsorption properties of tellurium oxide nanoparticles and graphene nanosheets prepared by Q-switched Nd-YAG pulsed laser. Journal of Nanostructures, 13(3): 889-897. https://doi.org/10.22052/JNS.2023.03.030

[31] Aziz, H.M., Al-Mamoori, M.H.K., Aboud, L.H. (2021). Synthesis and characterization of TiO_2-RGO nanocomposite by pulsed laser ablation in liquid (PLAL-method). Journal of Physics: Conference Series, 1818: 012206. https://doi.org/10.1088/1742-6596/1818/1/012206

[32] Al-Nafiey, A., Al-Mamoori, M.H.K., Alshrefi, S.M., Shakir, A.K., Ahmed, R.T. (2019). One step to synthesis (rGO/Ni NPs) nanocomposite and using to adsorption dyes from aqueous solution. Materials Today: Proceedings, 19(1): 94-101. https://doi.org/10.1016/j.matpr.2019.07.663

[33] Usman, A.K., Aris, A., Labaran, B.A., Darwish, M., Jagaba, A.H. (2022). Effect of calcination temperature on the morphology, crystallinity, and photocatalytic activity of ZnO/TiO_2 in selenite photoreduction from aqueous phase. Journal of New Materials for Electrochemical Systems, 25(4): 251-258. https://doi.org/10.14447/jnmes.v25i4.a05

[34] Ibrahim, N.M., Ahmad, H.S.M., Kadhim, E.J., Al-Joboury, W.M.R., Almamoori, G.S. (2025). Photocatalytic elimination of tetracycline from wastewater using immobilized titanium dioxide coated glass under sunlight. International Journal of Design & Nature and Ecodynamics, 20(6): 1313-1321. https://doi.org/10.18280/ijdne.200611